Time-Resolved Dynamic Light Scattering Study on Gelation and Gel-Melting Processes of Gelatin Gels

Masahiko Okamoto and Tomohisa Norisuye

Department of Polymer Science & Engineering, Kyoto Institute of Technology, Matsugasaki, Sakyo-ku, Kyoto 606-8585, Japan

Mitsuhiro Shibayama*

Neutron Scattering Laboratory, Institute for Solid State Physics, The University of Tokyo, Tokai, Naka-gun, Ibaraki 319-1106, Japan

Received April 27, 2001

ABSTRACT: The gelation and gel-melting processes have been investigated by time-resolved dynamic light scattering for gelatin aqueous solutions (1) during both cooling and heating processes with a fixed rate (0.10 °C/min) and (2) after quenching from 50 to 10 °C. In both cases, the gelation threshold was clearly observed as (i) appearance of strong fluctuations in scattered intensity, (ii) a power-law behavior in the time−intensity correlation function (ICF), and (iii) deviation of the initial amplitude of ICF. The physical implication of these phenomena is discussed.

Introduction

Gelatin has long been an intriguing material due to its unique mechanical properties with biological origin. It is needless to mention that one of the prominent properties of gelatin is the capability of gelation and gel melting with temperature. In the 1950s, Eldridge and Ferry proposed a van't Hoff equation for the thermodynamics on the cross-linking process of gelatin.[1] Studies on gelatin have also been carried out from the viewpoints of structure[2] and optical rotation[3] as well as dynamic light scattering.[4] However, the processes of gelation have been mostly investigated by rheological methods.[5−9] These rheological studies provided useful information about the sol−gel transition. The critical viscoelastic properties of gelatin at the gel point were discussed by Michon et al.[7,10,11]

Recently, Ren and Sorensen reported that the gelation threshold of gelatin can be detected as a drastic change in the time−intensity correlation function obtained by dynamic light scattering (DLS).[12,13] They showed that the slow mode diverges, and a power-law behavior appears at the sol−gel transition. In the case of chemical gels, such as poly(*N*-isopropylacrylamide) gels[14,15] and silica gels,[16] we demonstrated that the gelation threshold can be determined by characteristic changes in the four quantities obtained by DLS, i.e., the scattered intensity, I, the time−intensity correlation function, $g^{(2)}(\tau)$, the decay time distribution function, $G(\Gamma)$, and the initial amplitude of ICF, σ_I^2, where Γ is the decay rate. At the gelation threshold, strong fluctuations appear in I, $g^{(2)}(\tau) - 1$ exhibits a power-law behavior at large τ, a characteristic broadening takes place in $G(\Gamma)$, and σ_I^2 deviates from unity. All of these features are related to nonergodic nature of gels[17] and a self-similar distribution of the cluster size at the gel point.[18] The objective of this paper is to examine whether or not the above criteria for gel point are also applicable to thermoreversible biological gels, such as gelatin, of which the gelation mechanism is rather sophisticated due to participation of coiling of helical chains of protein molecules, hydrogen bonding, and so on.

Experimental Section

Samples. Alkali-treated gelatin (type B; lot no. P-3201) was kindly supplied by Nitta Gelatin Co., Osaka, Japan, which was used without further purification. The weight-average molecular weight was 1.45×10^5. The gelatin was immersed in distilled water for 10 min, followed by dissolution at 50 °C for 1 h. After filtration with a 0.45 μm Micropore filter, the gelatin solution was poured in an 8 mm test tube. In the case of constant cooling and heating experiments, the gelatin concentration was fixed to be 2.5 wt %. On the other hand, the concentrations of 0.20, 0.35, 0.5, and 2.5 wt % were chosen for time-resolved DLS experiments after temperature quenching.

DLS. Dynamic light scattering (DLS) studies were carried out on a static/dynamic compact goniometer (SLS/DLS-5000), ALV, Langen, Germany. The wavelength of the incident laser was 632.8 nm (He−Ne laser) with a power of 22 mW. The temperature of the sample was cooled by temperature-controlled circulating water with a constant cooling rate (0.10 °C/min). During the cooling process DLS measurements were conducted every 30 s at the scattering angle of 90° in order to investigate time evolution of the gelation process. After reaching 10 °C, the sample was aged for 60 min and then was heated at the same rate from 10 to 50 °C. To examine the wavenumber dependence of relaxation modes, DLS measurements were also carried out at various scattering angles from 45° to 150°. Similarly to the cooling process, a gel-melting process was monitored with the DLS. For time-resolved DLS measurements, the temperature of gelatin solutions was quickly changed from 50 to 10 °C, and data acquisition was made every 30 s.

Results and Discussion

Gelation during Constant Cooling/Heating Process. Figure 1 shows (a) the time evolution of the time-average scattered intensity, $\langle I \rangle_T$, of a 2.5 wt % gelatin solution during cooling process from 50 to 10 °C and (b) the corresponding temperature variation with time, t. The scattering angle was 90°. At the beginning, $\langle I \rangle_T$ remains constant up to $t = 250$ min but started to increase with large fluctuations at $t > 300$ min. These fluctuations and the increase in $\langle I \rangle_T$ are ascribed to an

* To whom correspondence should be addressed.

10.1021/ma010734b CCC: $20.00
Published on Web 10/27/2001

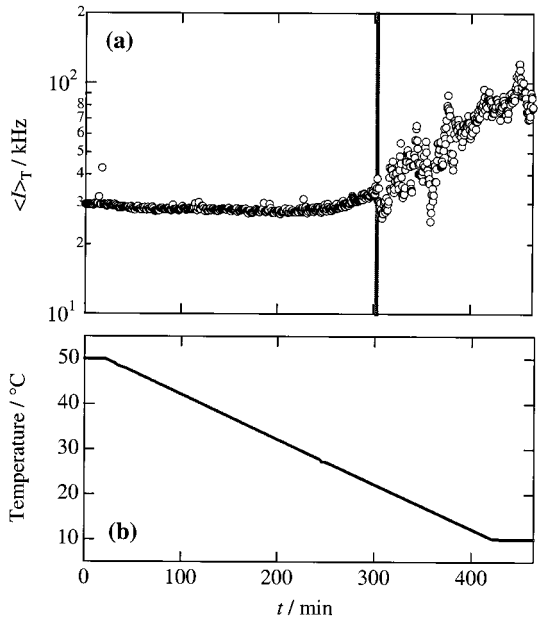

Figure 1. (a) Variation of the scattered intensity, $\langle I \rangle_T$, and (b) sample temperature with time, t, for a gelatin gel with 2.5 wt % during cooling process from 50 to 10 °C at a rate of 0.10 °C/min. The shaded line indicates where fluctuations in $\langle I \rangle_T$ appear.

emergence of nonergodicity[17] as the system becomes a gel.[14] Evidences of gelation can be examined by analyzing the time−intensity correlation function as discussed below.

The dynamics of polymer solutions can be studied with time−intensity correlation function, $g^{(2)}(\tau)$, which is given by[19]

$$g^{(2)}(\tau) \equiv g^{(2)}(\tau;q) = \frac{\langle I(0;q)\, I(\tau;q)\rangle_T}{\langle I(0;q)\rangle_T^{\,2}} = |g^{(1)}(\tau;q)|^2 + 1 \quad (1)$$

where $I(\tau;q)$ is the scattered intensity at time τ with respect to $\tau = 0$ and the scattering vector q, and $\langle ... \rangle_T$ denotes time average. $g^{(1)}(\tau)$ is the scattering field time correlation function given by

$$g^{(1)}(\tau) = \int_0^\infty G(\Gamma) \exp(-\Gamma\tau)\, d\Gamma \quad (2)$$

$G(\Gamma)$ is the characteristic decay time distribution function, where Γ^{-1} is the characteristic decay time. Figure 2 shows the time evolution of the time−intensity correlation function (ICF), $g^{(2)}(\tau) - 1$, obtained at 90° for a 2.5 wt % gelatin solution. The temperature was lowered with the constant cooling rate (0.10 °C/min). As shown here, the ICF becomes broader with time, and the tail of the ICF becomes larger with time until $t \approx 303$ min. However, after $t = 303$ min, the tail becomes shorter with time. According to the literature,[20] ICFs for sol and gel can be described by the following functions:

$$g_T^{(2)}(\tau) - 1 \approx \sigma_I^{\,2}\{A \exp(-Dq^2\tau) + (1 - A) \times \exp[-(\tau/\tau_c)^\beta]\}^2 \quad \text{(sol)} \quad (3)$$

$$g_T^{(2)}(\tau) - 1 \approx \sigma_I^{\,2}\{A \exp(-Dq^2\tau) + (1 - A)[1 + (\tau/\tau^*)]^{(n-1)/2}\}^2 \quad \text{(gel point)} \quad (4)$$

where σ_I^2 is the initial amplitude of ICF, A is the fraction of the collective diffusion mode, and D is the diffusion coefficient of the fast mode. τ_c is the characteristic time for the stretched exponential mode, and β is the stretched exponent. τ^* is the characteristic time where the power law behavior appears, and n ($0 < n < 1$) is the fractal dimension of scattered photons.[20] Analyses of sols and gels with eqs 3 and 4 are quite successful for silica gels[20] and poly(vinly alcohol)/Congo Red complex gels.[21,22] However, these equations could not apply to this system due to the presence of a large-τ cutoff. An example is given for the case with $t = 303.0$ min in Figure 2 (the deviation from the dashed line). That is, the power-law fit does not work for $t > 10^2$ ms. Hence, we introduced an alternative function given by

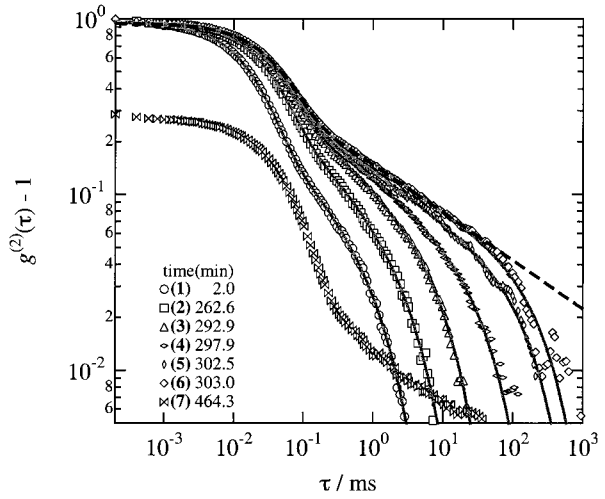

Figure 2. Time−intensity correlation functions, $g^{(2)}(\tau) - 1$, for a gelatin aqueous system with 2.5 wt % during cooling process. The data are fitted with either eq 3 (solid lines) or eq 5 (dashed line). The gelation point is determined to be 303.0 min. After passing the gelation time, the initial amplitude of $g^{(2)}(\tau) - 1$ deviates from unity.

$$g^{(2)}(\tau) - 1 \approx \sigma_I^{\,2}\left\{A \exp(-Dq^2\tau) + \frac{1 - A}{\{1 + (\tau/\tau^*)\}^{(1-n)/2}} \exp(-\tau/\tau_{max})\right\}^2 \quad (5)$$

where τ_{max} is the large-τ cutoff of ICF. The solid lines indicate the fit with this function.

Figure 3 shows the time variations of (a) τ^*, τ_{max} and (b) A, n. These indicate that the dynamics, i.e., the fast and slow modes, is unchanged during the cooling process, and only τ_{max} becomes larger near the gelation threshold. The physical meaning of this cutoff is related to a finite-rate cooling of gels since such a cutoff does not appear in ICF for aged gels as will be shown in Figure 9.

Figure 4 shows a series of decay time distribution functions, $G(\Gamma)$, obtained by inverse Laplace transform of ICF. Even in the sol state ($t = 0$ min; $T = 50$ °C), it is clear that the system consists of a few different modes, namely, the fast, middle, and slow modes. The fast mode is known to be collective mode of entangled polymer chains, which corresponds to the first term of the right-hand side of eq 5. On the other hand, the slow mode, corresponding to the second term in eq 5, is assigned to be the translational diffusion mode of clusters. The middle mode seems to be an artifact of inverse Laplace transform, the discussion of which is beyond of the scope of this work. By gelation time goes, $G(\Gamma)$ is broadened with a shift of the peak position toward larger τ.

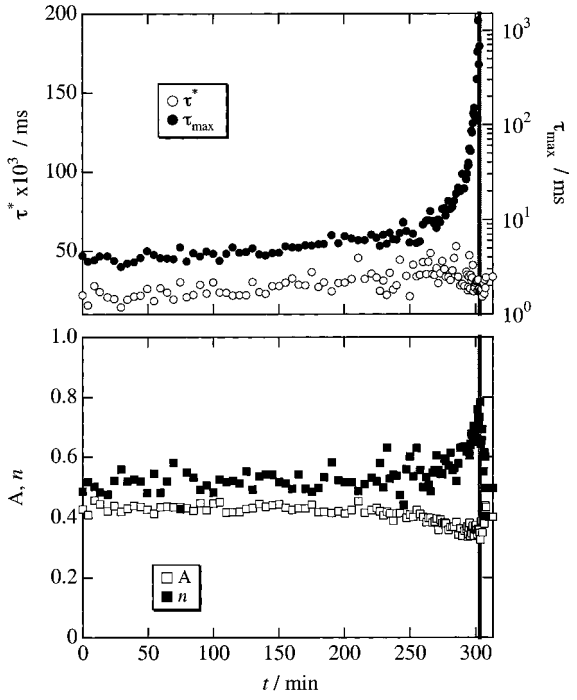

Figure 3. Variations of the fitted parameters with time during the cooling process of 2.5 wt % gelatin aqueous system: (a) the characteristic time for the power law, τ^*, and the large-τ cutoff, τ_{max}, and (b) the fraction of collective diffusion mode, A, and the power-law exponent, n.

However, after reaching $t = t_{gel}$ (≈303.0 min), the slow mode disappears. $G(\Gamma)$ shrinks back to a narrow shape, even narrower than the initial state ($t \approx 4.0$ min). $G(\Gamma)$ indicates that the dynamics is dominated by the collective mode (gel mode) in the late stage of gelation.

Figure 5 shows the time variation of (a) $\langle I \rangle_T$ and (b) the initial amplitude of ICF, $\sigma_I^2 \equiv g^{(2)}(\tau=0) - 1$. The time-average scattered intensity, $\langle I \rangle_T$, was monitored at the scattering angle of 90°. As shown here, both of these variables indicate drastic changes at one specific time ($t \approx 303.0$ min), i.e., (a) an appearance of fluctuations in $\langle I \rangle_T$ and (b) a suppression of σ_I^2 from unity. According to our previous studies on chemical gels,[14−16,23] this specific time is deduced to be the time at gelation threshold, t_{th}. Accordingly, the gelation temperature T_{gel} = 21.9 °C was determined via Figure 1b. It is clear from this demonstration that TRDLS allows one to determine the gelation threshold.

Similarly to the gelation process, the gel-melting process was investigated by time-resolved DLS for a gel at 10 °C heated with a constant rate of 0.10 °C/min to 50 °C. The variations of the variables, such as, $\langle I \rangle_T$, $g^{(2)}(t=0) - 1$, σ_I^2, and $\langle \tau \rangle$, were just opposite to those in Figures 1, 2, and 4, except the difference in the gel-melting temperature. The gel-melting temperature was determined to be 30.0 °C, which is significantly higher than the gelation temperature (21.9 °C). Note that a pioneering study on gelation and gel melting of gelatin was reported by Boedtkaer,[2] who pointed out the presence of hysteresis. The difference between these temperatures indicates the presence of hysteresis as systematically studied by Pouradier[24] and by te Nijenhuis.[25]

Figure 6 shows scattering-angle dependence of ICFs for gels at the gelation theshold in the cooling process. A power-law fit with eq 4, indicated with solid line, was carried out, from which the power-law exponent n was evaluated. Figure 7 shows the q^2 dependence of n and

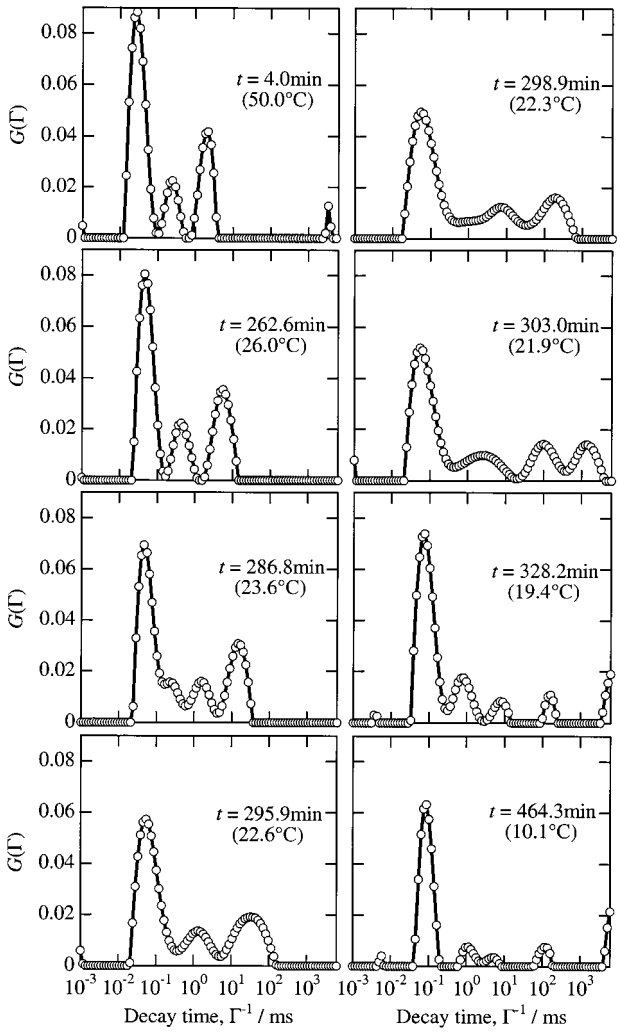

Figure 4. A series of decay time distribution functions, $G(\Gamma)$, for 2.5 wt % gelatin solution during cooling process with the rate of 0.1 °C/min, where Γ^{-1} is the decay time.

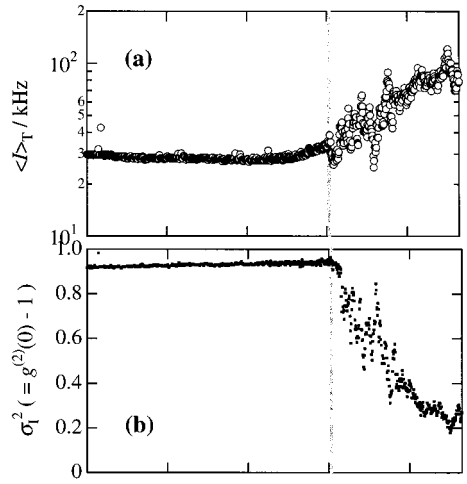

Figure 5. Time evolutions of (a) the scattered intensity $\langle I \rangle_T$ and (b) the initial amplitude of ICF for 2.5 wt % gelatin solution during gelation process by cooling at a rate of 0.1 °C/min.

the gelation temperature, T_{gel}. Note that these values were determined independently for freshly made samples at different scattering angles. It was found that T_{gel} was uniquely determined to be about 22.0 °C independent of q, as it should be. The power-law experiment n was

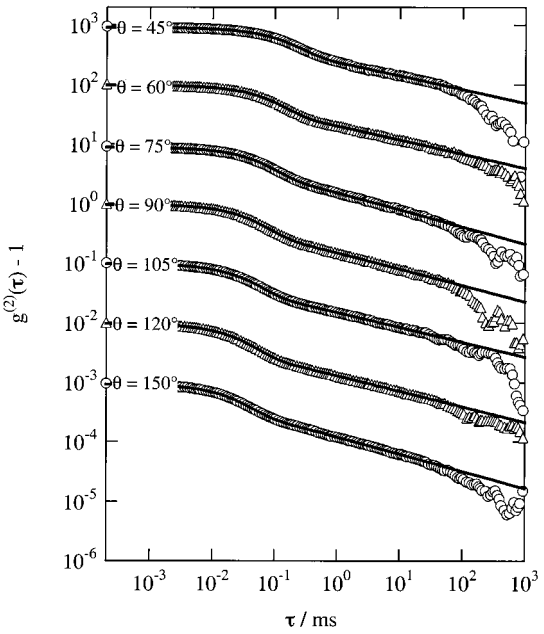

Figure 6. Scattering angle dependence of ICFs for 2.5 wt % gelatin solution at the gelation threshold. Each curve was obtained individually from gelatin gels at the threshold prepared from fresh 2.5 wt % gelatin aqueous solutions.

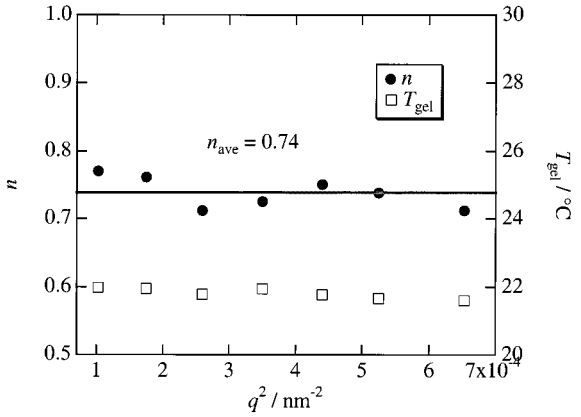

Figure 7. q^2 dependence of the power-law exponent, n, and gelation temperature, T_{gel}.

also independent of q, and the value was 0.74, which is close enough to the viscoelastic exponent obtained by Michon et al. (0.6−0.71, dependent on polymer concentration and temperature).[10] Note that the limiting value of n for the gel in the cooling process also gives a similar value at the gelation point (see Figure 3). The q independence of n was again confirmed in this study as well as those reported elsewhere,[26] which is inconsistent with the result reported by Ren et al.[12,13] Since the exponent is related to the viscoelastic exponent as discussed by Doi and Onuki,[27] q independence seems to be more reasonable.

Gelation Process after Temperature Quench. It is well-known that it takes a rather long time for

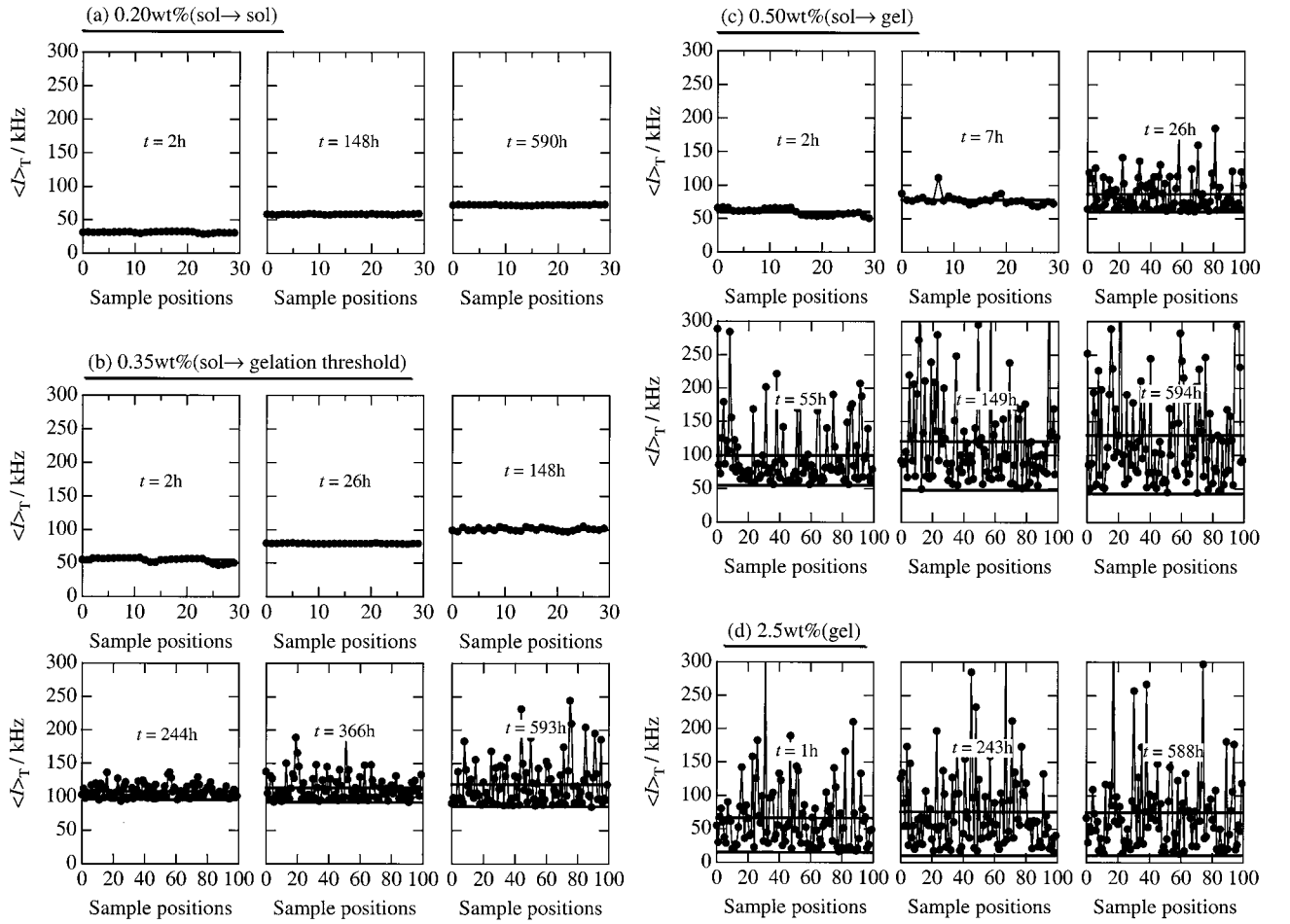

Figure 8. Time evolutions of speckle patterns for gelatin aqueous systems with (a) 0.20, (b) 0.35, (c) 0.50, and (d) 2.5 wt %. The horizontal solid and dashed lines indicate the ensemble average scattered intensity, $\langle I \rangle_E$, and time average scattered intensity, $\langle I \rangle_T$.

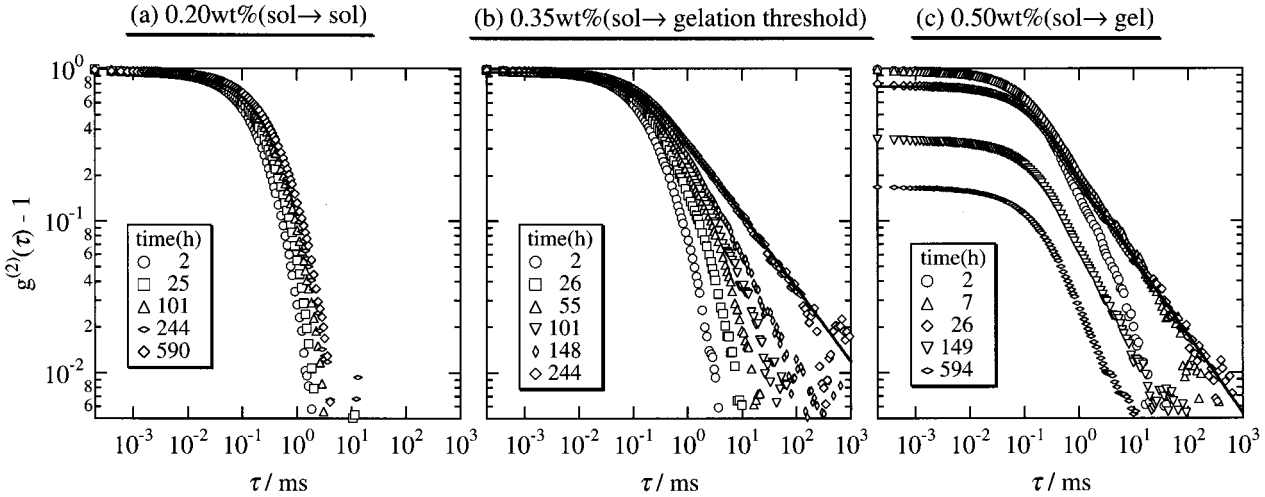

Figure 9. Time evolutions of ICFs for gelatin aqueous systems with (a) 0.20, (b) 0.35, and (c) 0.50 wt %. The solid lines in (b) and (c) denote the results of a power-law fit.

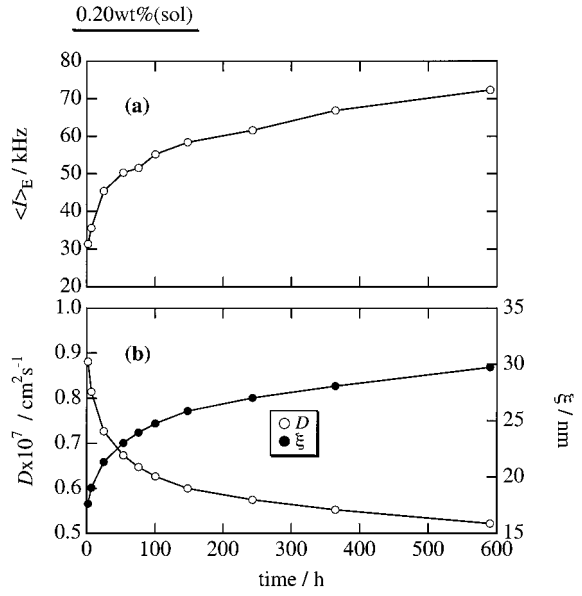

Figure 10. Time evolutions of (a) $\langle I \rangle_E$ and (b) D (and ξ) for 0.2 wt % gelatin.

biological gels to reach equilibrium. For example, Meuier et al. reported that a 12 h maturation was not long enough for equilibration of κ-carrageenan gels.[28] te Nijenhuis[25,29] also discussed the mechanical properties of gelatin gel during aging. Similarly, a kinetics of gelation of gels was investigated by optical rotation.[30] To understand the kinetics of gelation more comprehensively, we chose four gelatin concentrations which cover the sol−gel transition border (0. 35 wt %) at equilibrium state (i.e., $t \rightarrow \infty$) at 10 °C, i.e., 0.20, 0.35, 0.50, and 2.5 wt %. The gelatin with 0.20 wt % never gels at 10 °C. On the other hand, the 0.50 wt % gelatin exhibits a slow gelation of the order of hours. The 2.5 wt % sample gels instantly by quenching to 10 °C.

Figure 8 shows time evolution of speckle patterns for (a) 0.20, (b) 0.35, (c) 0.50, and (d) 2.5 wt % gelatin aqueous systems. As shown in Figure 8a, the 0.20 wt % gelatin shows no speckle formation even for $t = 590$ h although $\langle I \rangle_T$ ($\equiv \langle I \rangle_E$) slightly increases with t. In the case of the 0.35 wt % gelatin, a speckle pattern appears at $t = 244$ h, and $\langle I \rangle_E$, denoted by the horizontal solid line, increases with t. The gelation time is shortened by increasing gelatin concentration as shown in Figure 8c.

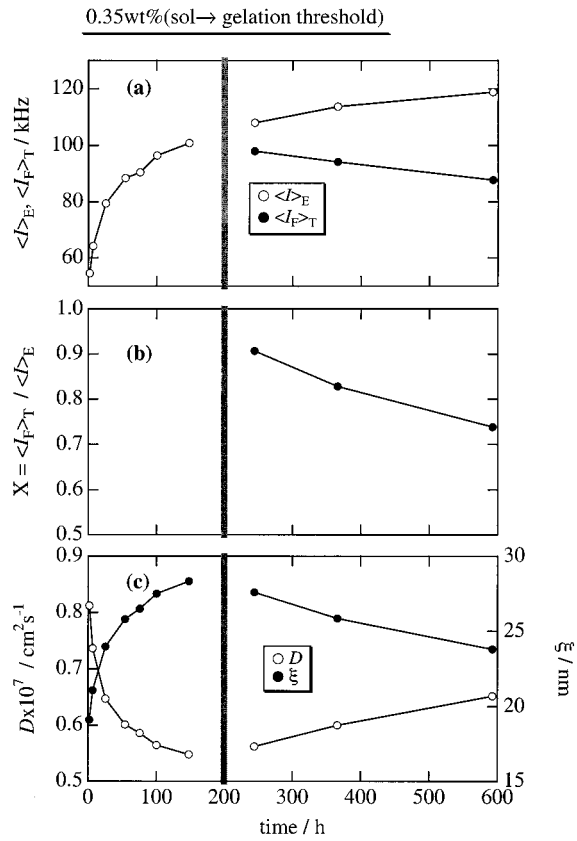

Figure 11. Time evolution of the DLS parameters (a) $\langle I \rangle_E$ and $\langle I_F \rangle_T$, (b) the fraction of the dynamic fluctuations to the scattered intensity, X, and (c) D (and ξ) for 0.35 wt % gelatin. The shaded lines indicate the gelation threshold.

In the case of the 2.5 wt % gelatin, a speckle pattern appears just after quenching (see Figure 8d). Therefore, it is clear that the gelation time of gelatin aqueous solutions at a fixed temperature is strongly dependent on the gelatin concentration.

Figure 9 shows the time course of ICFs of gelatin solutions of (a) 0.20, (b) 0.35, and (c) 0.50 wt %. As shown in Figure 9a, ICFs for the 0.20 wt % gelatin do not change significantly with time and can be more or less fitted with a single-exponential function. The relaxation is assigned to be translational diffusion of clustered gelatin molecules. A more detailed analysis

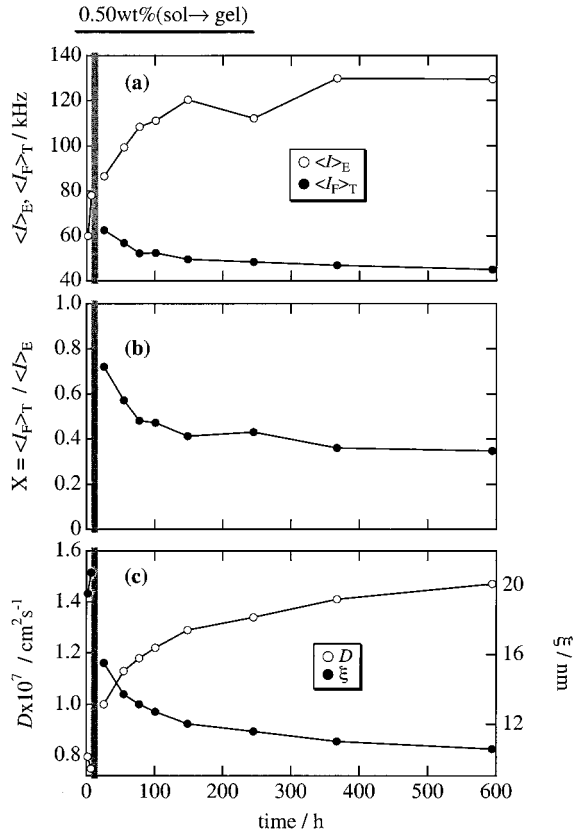

Figure 12. Time evolution of the DLS parameters (a) $\langle I \rangle_E$ and $\langle I_F \rangle_T$, (b) the fraction of the dynamic fluctuations to the scattered intensity, X, and (c) D (and ξ) for 0.50 wt % gelatin. The shaded lines indicate the gelation threshold.

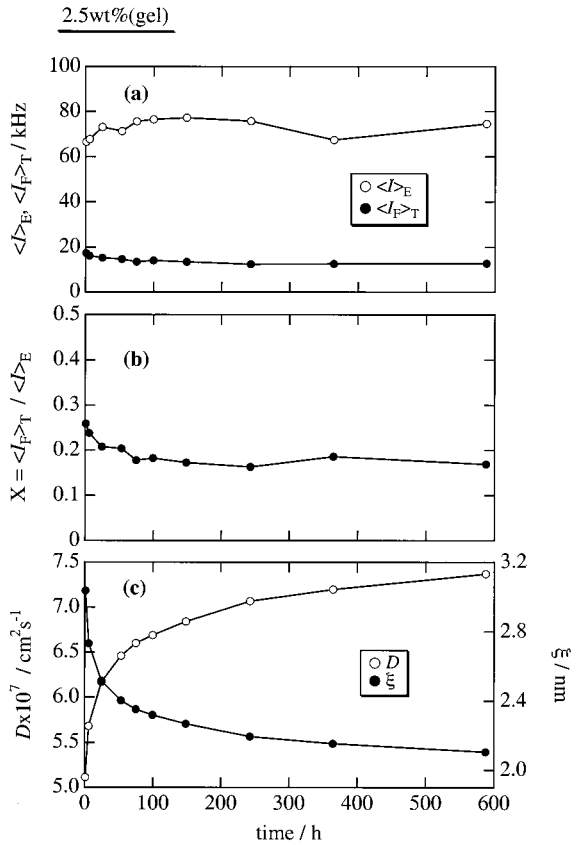

Figure 13. Time evolution of the DLS parameters (a) $\langle I \rangle_E$ and $\langle I_F \rangle_T$, (b) the fraction of the dynamic fluctuations to the scattered intensity, X, and (c) D (and ξ) for 2.5 wt % gelatin.

is given elsewhere.[26] A transition from a stretched exponential behavior (i.e., up to 148 h) to a power-law behavior (244 h) is clearly observed for the 0.35 wt % gelatin (Figure 9b). It is noteworthy that the power-law behavior does not accompany any large-τ cutoff observed in the cooling process (see Figure 2). Furthermore, the time at which this power-law behavior appears is consistent with the time where a speckle pattern appears (see Figure 8b). In the case of the 0.50 wt % gelatin, the system undergoes a sol-to-gel transition, and a power-law behavior appears at the gelation threshold. For further aging, the initial amplitude of ICF, i.e., σ_I^2, decreases from unity, which reflects the ergodic-to-nonergodic transition. Therefore, it is confirmed that the four methods of determination of gelation proposed elsewhere[16] can be applied to the gelatin aqueous system.

Figure 10 shows the variations of (a) $\langle I \rangle_E$ and (b) the diffusion coefficient D with time after temperature quench for gelatin solutions of 0.20 wt %, where D is defined by

$$D = -\frac{1}{2q^2}\frac{\partial}{\partial \tau}\ln[g^{(2)}(\tau) - 1]|_{\tau=0} \qquad (6)$$

It is surprising that it takes a rather long time (more than 600 h) for gelatin to attain a structural equilibration. This may be one of the characteristic features of biological gels. Clustering by aging made D decrease. From the value of D, the correlation length, ξ, i.e., a spatial length scale, such as the mean value of the cluster (for sols) or mesh size (for gels), can be estimated via

$$\xi = \frac{kT}{6\pi\eta D} \qquad (7)$$

Indeed, ξ increases with time due to clustering.

By conducting intensity correlation function analysis on all of the data points in the speckles, the time-fluctuating component in the scattered intensity, $\langle I \rangle_T$, was extracted from $\langle I \rangle_T$, and the collective diffusion coefficient, D, was evaluated, whose analysis is described elsewhere.[31−33] Figures 11 and 12 show the variations of (a) $\langle I_F \rangle_T$ and $\langle I \rangle_E$, (b) the ratio of the dynamic component to the total scattered intensity, X ($\equiv \langle I_F \rangle_T / \langle I \rangle_E$), and (c) D and ξ for the 0.35 and 0.50 wt % systems. The vertical shaded lines indicate the gelation time. While $\langle I \rangle_E$ keeps increasing with time, $\langle I_F \rangle_T$ decreases with time as a result of suppression of dynamic fluctuations after gelation point. The increase in $\langle I \rangle_E$ may suggest that cross-links are progressively formed with time, resulting in an increase in the degree of inhomogeneity. This is why ξ, i.e., a mesh size, decreases with time. A similar result was reported by Djabourov et al.[30] The gelation time depends on the gelatin concentration and shifts to a low value with increasing gelatin concentration.

Figures 13 shows the variations of (a) $\langle I_F \rangle_T$ and $\langle I \rangle_E$, (b) $\langle I_F \rangle_T / \langle I \rangle_E$, and (c) D and ξ for the 2.50 wt % system. In this case, $\langle I_F \rangle_T$, $\langle I \rangle_E$, and X are rather invariant with t, indicating that cross-links are instantaneously formed after T-jump. On the other hand, the gradual increase in D and the decrease in ξ with t suggest a progressive formation of cross-links.

Conclusion

The transition threshold of gelation as well as gel melting was successfully determined for the gelatin aqueous systems during cooling and heating processes. The transition threshold was characterized by (1) an appearance or annihilation of strong fluctuations in the scattered intensity, (2) a power-law behavior in ICF, and (3) a suppression of the initial amplitude of ICF. It was found that there exists a hysteresis in the gelation and gel-melting processes with the temperature gap of about 8 °C (for the case of gelatin gel with $C = 2.5$ wt %). A modified power-law function with a large-τ cutoff analysis was necessary to analyze the gelatin during the cooling and heating process. It was also found that the power-law exponent, n, is q independent and is around 0.74 for $C = 2.5$ wt % in this particular case.

The gelation process was also investigated after temperature quench from 50 to 10 °C. The sol−gel transition behavior of gelatin at 10 °C was quantitatively investigated for aged gelatin solutions, and a decomposition of the frozen and dynamic component was conducted. A departure of the ensemble average scattered intensity, $\langle I \rangle_E$, from $\langle I_F \rangle_T$, and a divergence of D at the gelation threshold were observed. It was found that it takes more than a few hundred hours to reach equilibrium. A clear power law was observed for the aged gel.

Acknowledgment. This work is partially supported by the Ministry of Education, Science, Sports and Culture, Japan (Grant-in-Aid, 12450388 and 13031019 to M.S.).

References and Notes

(1) Eldridge, B. J.; Ferry, J. D. *J. Phys. Chem.* **1954**, *58*, 992.
(2) Boedtkaer, H.; Doty, P. *J. Phys. Chem.* **1954**, *58*, 968.
(3) Harrington, W. F.; Rao, N. V. *Biochemistry* **1970**, *9*, 3714.
(4) Djabourov, M.; Leblond, J.; Papon, P. *J. Phys. (Paris)* **1988**, *49*, 333.
(5) te Nijenhuis, K. *Colloid Polym. Sci.* **1981**, *259*, 522.
(6) Cuvelier, G.; Launay, B. *Macromol. Chem., Macromol. Symp.* **1990**, *40*, 23.
(7) Amis, E. J.; Hodgson, D. F.; Yu, Q. *Polym. Prepr.* **1991**, *32*, 447.
(8) Huang, H.; Sorensen, C. M. *Phys. Rev. E* **1996**, *53*, 5075.
(9) Peyrelasse, J.; Lamarque, M.; Habas, J. P.; Boedtkaer, H.; Bounia, N. E. *Phys. Rev. E* **1996**, *53*, 6126.
(10) Michon, C.; Cuvelier, G.; Launay, B. *Rheol. Acta* **1993**, *32*, 94.
(11) Hsu, S.-H.; Jamieson, A. M. *Polymer* **1993**, *34*, 2602.
(12) Ren, S. Z.; Shi, W. F.; Zhang, W. B.; Sorensen, C. M. *Phys. Rev. A* **1992**, *45*, 2416.
(13) Ren, S. Z.; Sorensen, C. M. *Phys. Rev. Lett.* **1993**, *70*, 1727.
(14) Norisuye, T.; Shibayama, M.; Nomura, S. *Polymer* **1998**, *39*, 2769.
(15) Norisuye, T.; Takeda, M.; Shibayama, M. *Macromolecules* **1998**, *31*, 5316.
(16) Norisuye, T.; Shibayama, M.; Tamaki, R.; Chujo, Y. *Macromolecules* **1999**, *32*, 1528.
(17) Pusey, P. N.; van Megen, W. *Physica A* **1989**, *157*, 705.
(18) Stauffer, D. *Introduction to Percolation Theory*; Taylor & Francis: London, 1985.
(19) Chu, B. *Laser Light Scattering*, 2nd ed.; Academic Press: New York, 1991.
(20) Martin, J. E.; Wilcoxon, J.; Odinek, J. *Phys. Rev. A* **1991**, *43*, 858.
(21) Ikkai, F.; Shibayama, M. *Phys. Rev. Lett.* **1999**, *82*, 4946.
(22) Shibayama, M.; Tsujimoto, M.; Ikkai, F. *Macromolecules* **2000**, *33*, 7868.
(23) Takata, S.; Norisuye, T.; Tanaka, N.; Shibayama, M. *Macromolecules* **2000**, *33*, 5470.
(24) Pouradier, J. *J. Chim. Phys.* **1971**, *10*, 1547.
(25) te Nijenhuis, K. *Colloid Polym. Sci.* **1981**, *259*, 1017.
(26) Shibayama, M.; Okamoto, M. *J. Chem. Phys.* **2001**, *115*, 4285.
(27) Doi, M.; Onuki, A. *J. Phys. II* **1992**, *2*, 1631.
(28) Meunier, V.; Nicolai, T.; Durand, D.; Parker, A. *Macromolecules* **1999**, *32*, 2610.
(29) te Nijenhuis, K. *Adv. Polym. Sci.* **1997**, *130*, 1.
(30) Djabourov, M.; Leblond, J.; Papon, P. *J. Phys. (Paris)* **1988**, *49*, 319.
(31) Fang, L. *Macromolecules* **1991**, *24*, 6839.
(32) Shibayama, M.; Fujikawa, Y.; Nomura, S. *Macromolecules* **1996**, *29*, 6535.
(33) Shibayama, M. *Macromol. Chem. Phys.* **1998**, *199*, 1.

MA010734B